J Mater Sci (2007) 42:5490–5496
DOI 10.1007/s10853-006-0985-8

Effect of simultaneous substitution of La and Mn on dielectric behavior of barium titanate ceramic

**Om Parkash · Devendra Kumar · R. K. Dwivedi ·
K. K. Srivastava · Prakash Singh · Sindhu Singh**

Received: 12 May 2006 / Accepted: 21 September 2006 / Published online: 3 April 2007
© Springer Science+Business Media, LLC 2007

Abstract A few compositions in the valence compensated system $Ba_{1-x}La_xTi_{1-x}Mn_xO_3$ were synthesized by solid-state ceramic method to study the effect of co-doping lanthanum and manganese in equimolar amounts on dielectric behavior of $BaTiO_3$. Compositions with $x \le 0.10$ have shown solid solution formation. Compositions with $x \le 0.05$ are found to have tetragonal structure at room temperature while composition with $x = 0.10$ is cubic. Plots of relative dielectric constant, ε_r versus temperature for composition with $x = 0.01$ show dielectric anomalies around 376 ± 2, 264 ± 2 and 179 ± 2 K which correspond to cubic to tetragonal (T_{C-T}), tetragonal to orthorhombic (T_{T-O}) and orthorhombic to rhombohedral (T_{O-R}) transition, respectively, similar to $BaTiO_3$. Curie temperature has been found to decrease with increasing concentration of lanthanum and manganese simultaneously in barium titanate. The broadening in the dielectric peak at cubic to tetragonal (T_{C-T}) transition temperature increases with increasing x. For $x = 0.10$, only one anomaly at 100 K is observed in its ε_r versus T plots. The observation of this single anomaly may be due to pinching effect of the substitutions on the three phase transitions.

Om Parkash (✉) · D. Kumar · K. K. Srivastava ·
P. Singh · S. Singh
Department of Ceramic Engineering, Institute of Technology,
Banaras Hindu University, Varanasi 221 005, India
e-mail: opec_itbhu2003@yahoo.co.in

R. K. Dwivedi
Department of Physics, Jaypee Institute of Information
Technology, Noida 201307, India

Introduction

Most of the ceramic capacitors at present have compositions based on $BaTiO_3$, which is a well known ferroelectric material. Pure or undoped $BaTiO_3$ shows marked changes in the values of dielectric parameters particularly near its Curie temperature. This is an undesirable feature for its use as a thermally stable capacitor material. Its properties are modified by a wide variety of substitutions possible at barium or titanium sites independently or simultaneously. These substitutions can be isovalent or heterovalent. Extensive research work on the effect of isovalent substitutions on dielectric properties and transition temperatures of $BaTiO_3$ has been done during the last few decades [1–3]. The heterovalent substitutions at A or B sites cause charge imbalance and require creation of vacancies in A or B or oxygen sublattice or generation of holes to maintain electrical charge neutrality. It has been reported that for small concentration of La^{3+} substituted at Ba^{2+} sites, the charge neutrality is maintained by electronic compensation in accordance with $Ba^{2+}{}_{1-x}La^{3+}{}_xTi^{4+}{}_{1-x}Ti^{3+}{}_xO_3$ [1]. However, for larger concentration of La^{3+} ions, the excess donor charge on La^{3+} ions is compensated by Ti vacancies as represented by the formula $Ba_{1-x}La_xTi_{1-x/4}(V_{Ti})''''_{x/4}O_3$ [4]. It has been, reported that lanthanum doped $BaTiO_3$, prepared by calcination and sintering in O_2 atmosphere results in only insulating materials for low as well as high concentration of lanthanum [5, 6]. All these samples were prepared according to compositions based on, vacancies in Ti-sublattice similar to Jonker and Havinga [6].

When there is simultaneous substitution of La^{3+} on Ba^{2+} sites and Fe^{3+}, Co^{3+} and Ni^{3+} on Ti^{4+} sites in equimolar concentration, then it is expected that the charge compensation is maintained internally without requiring the creation of defects. Such solid solutions are termed as valence compensated solid solutions. During the last few years, attempts were made to synthesize and study such type of valence compensated solid solutions [7–12]. Compositions with $x \leq 0.05$ in the system $Ba_{1-x}La_xT_{1-x}Mn_xO_3$ (M = Co or Ni) exhibit interesting dielectric properties [13, 14]. Diffuse ferroelectric to paraelectric transition occurs in the Co doped system while it is fairly sharp in Ni doped system. Some work has been reported on co-doped $BaTiO_3$ with a view to use these compositions for multi-layer capacitors applications using Ni electrodes [15–17]. Saito et al. studied the effect of holmium substitution on the electrical, dielectric and microstructural properties of co-doped $(Ba_{1.01}Mg_{0.01})_{0.02}(Ti_{0.98}Zr_{0.02})O_2$. Takeuchi et al. studied the effect of firing atmosphere on the microstructure, grain growth, electrical resistivity, IR-absorption and ESR spectra of $BaTiO_3$ co-doped with La and Mn in (0.2 mol% La–O and 0.05 mol% Mn and 0.3 mol% La–O and 0.05 mol% Mn) and Gd–Fe co-doped $BaTiO_3$ with addition of B_2O_3 used as sintering aid [15, 16]. In the former case core shell structure was observed. In both these systems resistivity decreased when the samples were fired in Ar atmosphere. This was described to formation of oxygen vacancies formed due to loss of oxygen during sintering in Ar atmosphere. It is to be noted that in all these systems care was not taken to maintain the electrical charge neutrality. The aim of these investigations was to develop compositions suitable for MLC applications using Ni electrode.

In view of the above, it was considered worthwhile to investigate an analogous valence compensated $Ba_{1-x}La_xTi_{1-x}Mn_xO_3$ perovskite system. Simultaneous substitution of manganese and lanthanum in equimolar amount is expected to maintain charge neutrality internally without requiring creation of defects if all the Mn ions exist in the trivalent state. The effect of substitutions of lanthanum on the dielectric behavior of $BaTiO_3$ has been studied earlier [4–6]. No report is available as yet on the dielectric and electrical behavior of this system with simultaneous heterovalent substitutions in equal concentration. We have limited these studies upto $x = 0.50$ because of our interest in the dielectric properties.

$LaMnO_3$ is an antiferromagnetic material, having a Neel temperature of ~100 K. It has orthorhombic crystal structure [18, 19]. In view of the interesting and useful properties of the two end members viz. $BaTiO_3$ and $LaMnO_3$, it was considered worthwhile to study the possibility of formation of solid solution between them and investigate dielectric behavior of solid solution compositions. In this paper, the synthesis, crystal structure and dielectric behavior of the system $Ba_{1-x}La_xTi_{1-x}Mn_xO_3$ have been reported.

Experimental

Compositions with $x = 0.01$, 0.03, 0.05, 0.10, 0.20, 0.30 and 0.50 in the valence compensated system $Ba_{1-x}La_xTi_{1-x}Mn_xO_3$ have been prepared by solid-state ceramic method. Appropriate amounts of barium carbonate (purity ~ 99.5%), lanthanum oxalate (purity ~ 99.99%), titanium dioxide (purity ~ 99%) and manganese dioxide (purity ~ 99.99%), were weighed for these compositions and ball milled for 6 h using acetone. Mixed powders were dried and calcined in a platinum crucible at 1,250 °C for 8 h. Calcined powders were compacted under an optimum load in the form of cylindrical discs using 2% solution of PVA as binder. These pellets were heated slowly upto 500 °C and held at this temperature for an hour to burn off the binder completely. Then the temperature of the furnace was raised to 1,300 °C at a heating rate of 5 °C/m. After sintering, the furnace was cooled at a rate of 5 °C/m upto 600 °C and then it was switched off. One pellet in each of the compositions was crushed to fine powder and powder X-ray diffraction patterns were recorded using Rigaku X-Ray Diffractometer. Another pellet in each of these compositions was polished using emery papers of grade 1/0, 2/0, 3/0, 4/0 and 5/0 and by diamond paste of grade 3, 1 and 1/4 μm, respectively. These polished surfaces were thermally etched at 1,400 °C for 40 min and coated with Au–Pd alloy by sputtering. Scanning Electron Microscope Model No. JEOL SEM 800 was used to observe the microstructures. Two pellets of each composition were coated with Ag–Pd paint which was cured at 750 °C for 20 min. These samples were used for dielectric measurements using impedance analyzer [Type HP 4192A LF]. Dielectric measurements have been made during heating from liquid nitrogen temperature to 500 K for $x \leq 0.05$ and 600 K for $x = 0.10$ at a rate of 1.5 °C/m and then again during cooling at a rate of 1.5 °C/m, respectively. A few compositions have been characterized by ESR spectroscopy.

Crystal structure, density and microstructure

Attempts were made to synthesize compositions with $x = 0.01$, 0.03, 0.05, 0.10, 0.20, 0.30 and 0.50. X-ray diffraction patterns for the compositions with $x = 0.01$, 0.03, 0.05 and 0.10 have shown formation of single-phase solid solution. Compositions with $x > 0.10$ were found to have X-ray diffraction lines of the constituent oxides in their X-ray diffraction patterns. XRD data of single phase compositions have been indexed on the basis of tetragonal symmetry for $x \leq 0.05$ and cubic symmetry for $x = 0.10$. These materials are produced by high temperature solid-state diffusion controlled thermo-chemical process. Because of this the dodecahedral and octahedral sites are occupied randomly by Sr^{2+}, La^{3+} and Ti^{4+}, Mn^{3+}/Mn^{2+}, respectively. This will lead to an overall cubic symmetry in composition with $x = 0.10$. Lattice parameters have been determined using a program 'CEL'.

Typical microstructures for the compositions with $x = 0.01$ and 0.10 are shown in Fig. 1. Average grain size has been found to be in the range 1–4 μm for all the samples. Small grain size observed in these materials may be due to segregation of dopants at grain boundaries, which inhibit grain growth [20]. Lattice parameters, structure, average grain size and % porosity for all the samples are given in Table 1. ESR spectra of these materials (not shown) at 25 and 100 °C have shown that Mn ions exist mostly in +3 state {which do not give any ESR signal because it has even number (4) of 3d electrons} while a week signal due to Mn^{2+} appears. The value of 'g', spectroscopic splitting factor which measures the ratio of spin to orbital magnetic moment obtained at both these temperatures is 2.001. This value of 'g' corresponds to Mn^{2+} or $Mn^{2+}–2V_{\mathrm{O}}$ or $Mn^{2+}–V_{\mathrm{O}}^{\cdot\cdot}$ defect complexes, where V_{O} and $V_{\mathrm{O}}^{\cdot\cdot}$ represent singly and doubly positively charged oxygen vacancies [21]. But the possibility of the other states of manganese ions (Mn^{4+}) cannot be ruled out in these materials, which are present below the detection limit of the experimental facility.

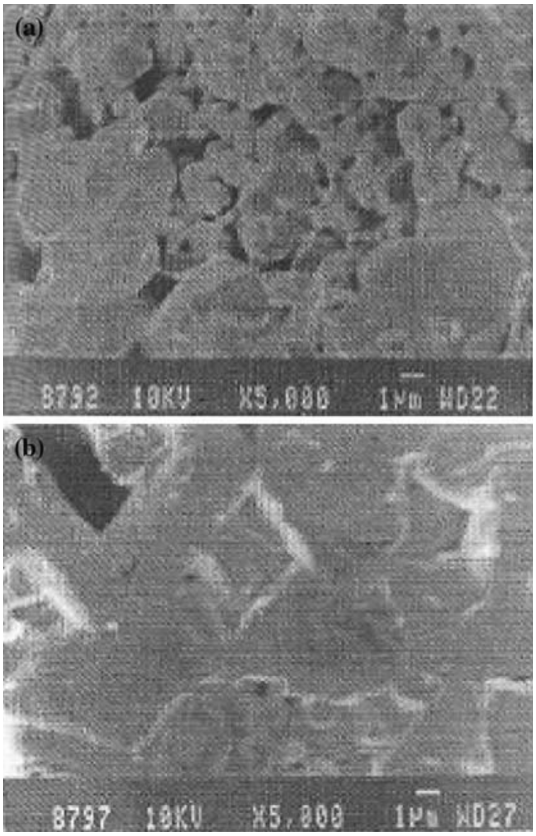

Fig. 1 Scanning electron micrographs of thermally etched surfaces of samples with x (a) 0.01 and (b) 0.10 in the system $Ba_{1-x}La_xTi_{1-x}Mn_xO_3$

Dielectric characterization

Dielectric measurements have been carried out as a function of frequency (100 Hz–1 MHz) in the temperature range 100–600 K. For the undoped specimen (i.e. $x = 0$), anomalies are observed in ε_r versus temperature plots (not shown) at 393, 278 and 185 K. These temperatures correspond to various phase transition temperatures in $BaTiO_3$ i.e. cubic to tetragonal ($T_{\mathrm{C–T}}$), tetragonal to orthorhombic ($T_{\mathrm{T–O}}$) and orthorhombic to rhombohedral ($T_{\mathrm{O–R}}$), respectively [1].

Plots of ε_r and D as a function of temperature at 1, 10 and 100 kHz for various compositions are shown in Fig. 2. For composition with $x = 0.01$, four dielectric anomalies have been observed at 378, 330, 270 and 190 K. Transition temperatures have been found to be independent of frequency (Fig. 2a) For $x = 0.03$ and 0.05, the dielectric anomalies corresponding to $T_{\mathrm{C–T}}$, $T_{\mathrm{T–O}}$ and $T_{\mathrm{O–R}}$ structural transitions have been found to shift to lower temperatures. The corresponding dielectric anomalies occur at 325, 230 and 150 K for $x = 0.03$ (Fig. 4b) and anomaly which occurs around 330 K for $x = 0.01$, appears as a very small deviation at around 300 K for this sample. For $x = 0.05$, these anomalies are found at around 300 and 190 K in addition to a small deviation at 250 K in ε_r versus T plots (Fig. 4c). The anomaly corresponding to $T \approx 185$ K in undoped $BaTiO_3$ could not be observed for this sample. This seems to occur at lower temperature, which is below temperature range of our measurement. Composition with $x = 0.10$ has shown one dielectric maxima at ~100 K at all the three frequencies (Fig. 2d). Another peak appears at ~490 K (at 1 kHz). At other frequencies it seems to appear at higher temperatures. An increasing value of dielectric constant with increasing temperature above 350 K has been observed in this sample. All these samples have shown frequency independent dielectric constant upto certain temperature T_a, which decreases with increasing concentration of dopants.

Plots of dissipation factor with temperature for these samples are shown in Fig. 2e–h. Dissipation factor initially remains independent of temperature upto certain temperature. Thereafter it increases with temperature. Compositions with $x = 0.01$ and 0.03 have shown an anomaly around $T_{\mathrm{C–T}}$ in these plots. The plots of higher compositions do not show any anomaly near this temperature.

The above results reveal that the peaks position in ε_r versus temperature plots shift to lower temperature with increasing concentration of lanthanum and manganese in $BaTiO_3$ (BT). The average decrease in Curie temperature

Table 1 Lattice parameters, structure, average grain size and % porosity for all the samples in the system $Ba_{1-x}La_xTi_{1-x}Mn_xO_3$

Composition (x)	Lattice parameters			Structure	Unit cell volume (m^3)	% Porosity	Av. grain size (μm)
	a (Å)	c (Å)	c/a				
0.00	3.997 ± 0.002	4.035 ± 0.004	1.009	Tetragonal	64.463×10^{-30}	7	–
0.01	3.994 ± 0.003	4.019 ± 0.003	1.006	Tetragonal	64.111×10^{-30}	17	1
0.03	3.990 ± 0.003	4.012 ± 0.003	1.005	Tetragonal	63.887×10^{-30}	15	2
0.05	3.989 ± 0.002	4.006 ± 0.002	1.004	Tetragonal	63.744×10^{-30}	16	3
0.10	3.986 ± 0.003	–	–	Cubic	63.330×10^{-30}	18	4

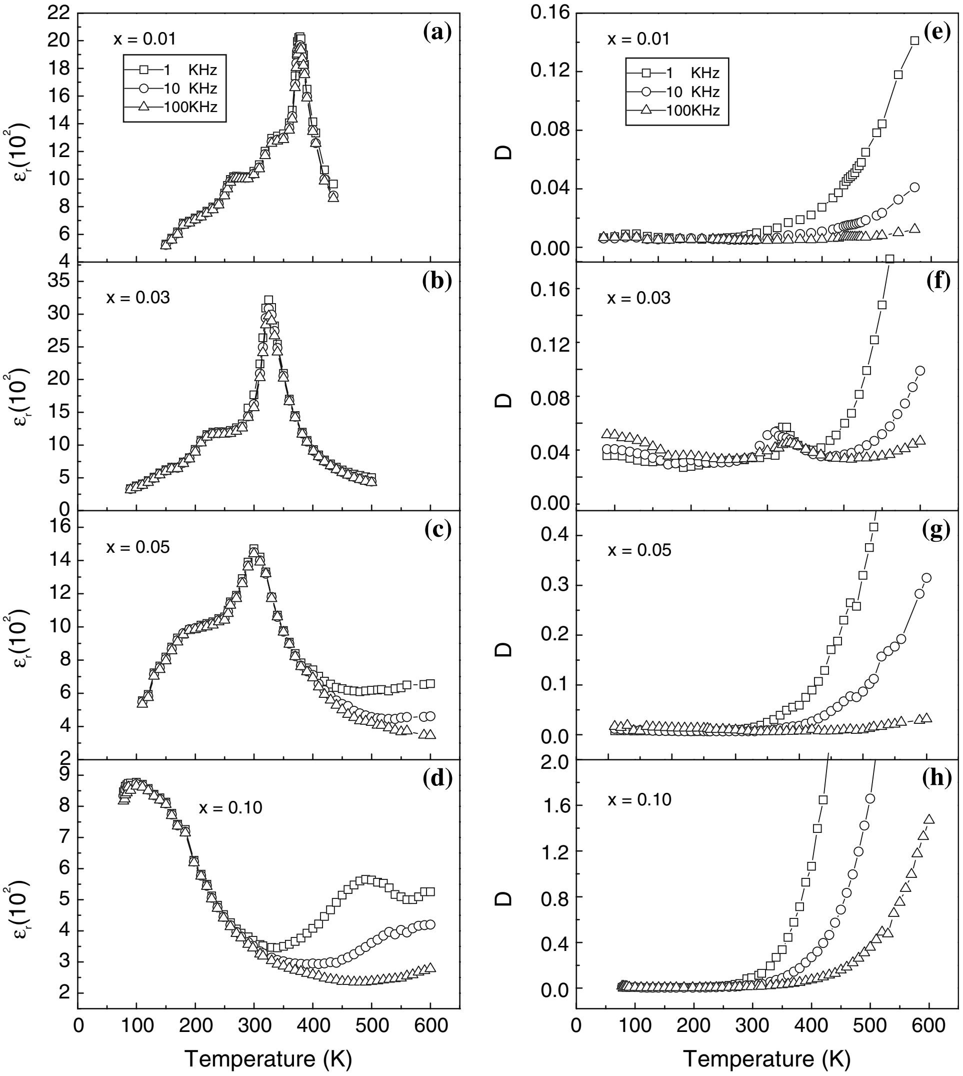

Fig. 2 Comparative plots of ε_r and D with temperature for various compositions (x) in the system $Ba_{1-x}La_xTi_{1-x}Mn_xO_3$

of BT has been found to be 20(±3) °C/at% substitution of lanthanum and manganese simultaneously upto $x = 0.05$. It is clear from the ε_r^{-1} versus temperature plots shown in Fig. 3 that these samples follow Curie–Weiss law above their Curie temperature, T_C.

The peak temperatures in ε_r versus T plots obtained during heating (T_C^H) and cooling (T_C^C) have been found to be different. The observed peak temperature during heating and cooling T_C^H and T_C^C and the difference ΔT for different compositions are given in Table 2. Composition with $x = 0.01$ has exhibited a wide thermal hysteresis between, heating and cooling cycle (Fig. 4) similar to undoped $BaTiO_3$. Thermal hysteresis decreases for compositions with higher values of x.

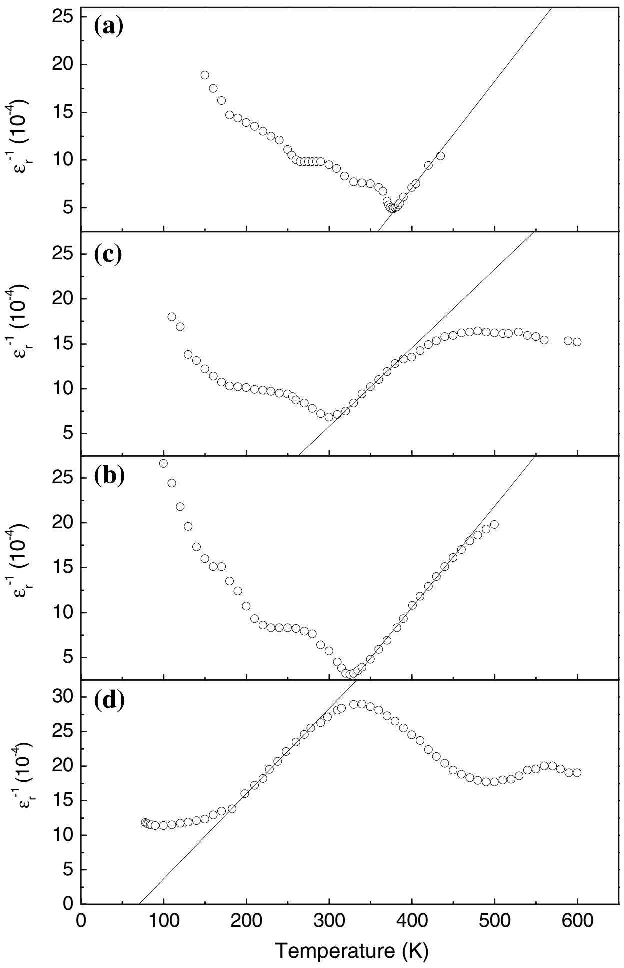

Fig. 3 Variation of inverse of dielectric constant, ε_r^{-1} with temperature for compositions x (a) 0.01, (b) 0.03, (c) 0.05 and (d) 0.10 in the system $Ba_{1-x}La_xTi_{1-x}Mn_xO_3$

Discussion

Paraelectric to ferroelectric transition in $BaTiO_3$ is known to occur at 393 K, where the structure changes from cubic to tetragonal. Other transitions from tetragonal to orthorhombic and from orthorhombic to rhombohedral have been reported to occur at 278 and 183 K, respectively [1].

Table 2 Ferroelectric–paraelectric transition temperatures, T_C in the system $Ba_{1-x}La_xTi_{1-x}Mn_xO_3$

Composition (x)	T_C^H	T_C^C	ΔT ($T_C^H - T_C^C$
0.01	378	370	8
0.03	325	320	5
0.05	300	296	4
0.10	100	–	–

T_C obtained during heating and cooling cycles (T_C^H and T_C^C) from dielectric measurements

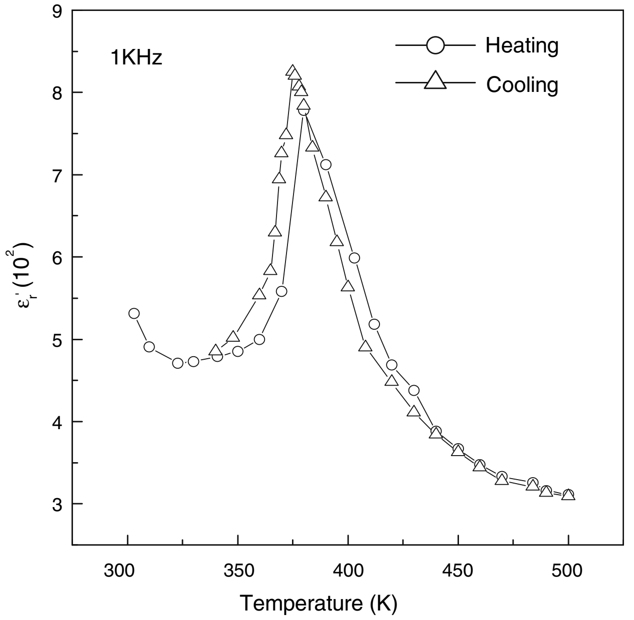

Fig. 4 Variation of dielectric constant, $\varepsilon_r^{/}$ with temperature at 1 kHz during heating and cooling cycle of the composition $Ba_{0.99}La_{0.01}Ti_{0.99}Mn_{0.01}O_3$

One possibility of shift of T_C on isovalent substitutions is that there will be some distortion due to different ionic radii of the dopants. But the possibility of shift of the Curie temperature, on the basis of the ionic radii, has been ruled out because it does not follow the order of shifting T_C for substitution of Ca, Sr and Pb in $BaTiO_3$ [22]. Strength of Pb–O and Ba–O bonding in $PbTiO_3$ and $BaTiO_3$, respectively, have been reported to influence their Curie temperature, respectively [23]. Since Pb–O bonding in $PbTiO_3$ is weaker than Ba–O bonding in $BaTiO_3$, therefore oxygen ion on fcc position is less tightly bound with surrounding Pb^{2+} ions in $PbTiO_3$ as compared to barium ion in $BaTiO_3$. The rigidity of the oxygen in this cage would decide the shift of Ti^{4+} ions, which would be more in $PbTiO_3$ as compared to $BaTiO_3$. The larger shift in Ti^{4+} ion causes larger polarization and hence the larger Curie temperature. This explains why $PbTiO_3$ has higher T_C than $BaTiO_3$.

If the effect of lanthanum substitution on T_C of $PbTiO_3$ and $BaTiO_3$ is to be considered then the bond strength of La–O with bond strength of Pb–O and Ba–O bonds should be compared. Substitution of La in $PbTiO_3$ reduces its T_C significantly [24]. This is due to the large difference in bond strength of Pb and La with oxygen being higher in case of La. Though lanthanum and barium lie close to each other in the periodic table, yet their bond strength with oxygen will be different, being more for La–O as compared to Ba–O due to higher valency of La^{3+} ions. This will increase the rigidity of oxygen lying in the face-centered positions in a cage formed by four corner Ba^{2+}/La^{3+} ions. This increase in rigidity will oppose the shift of Ti^{4+} from its body center position i.e. it will decrease shift of Ti^{4+} from center of symmetry and hence will reduce its Curie temperature. This is supported by results of Mazadyasni and Brown [25] who observed significant decrease of T_C on small addition of lanthanum to $BaTiO_3$.

Morrison et al [26] explained the lowering of T_C in lanthanum doped $BaTiO_3$ on the basis of concentration of A (Ba) and B (Ti) sites defects with increasing dopants concentration. According to these authors, the lowering of T_C with La substitution is firstly due to its smaller size as compared to Ba which makes tetragonal phase unstable and secondly due to creation of titanium vacancies which disrupt Ti–O–Ti linkages, responsible for ferroelectricity. Both these factors lead to lowering of T_C with increasing x in the system $Ba_{1-x}La_xTi_{1-x/4}(V_{Ti})^{//}_{x/4}O_3$.

Now let us consider the possible defects by manganese doping which acts as an acceptor on Ti-sites. It has already been mentioned that ESR spectra indicate that these samples contain manganese predominantly in Mn^{3+} states Mn^{3+} on Ti^{4+} site has an effective negative charge while Mn^{2+} on Ti^{4+} has two negative charges, respectively, viz $(Mn^{3+}{}_{Ti})^{/}$ and $(Mn^{2+}{}_{Ti})^{//}$. These ions in fully ionized state generate one and two holes, respectively, for lower concentration. For higher concentration electrical charge neutrality is achieved by oxygen vacancies. Traces of Mn^{4+} may also be present. Mn^{3+} ion on Ti^{4+} site acts as acceptor with one effective negative charge. At higher concentration, these are compensated by oxygen vacancies [1].

The other major defects present in these materials are oxygen ion vacancies similar to that in the $Sr_{1-x}La_xTi_{1-x}Co_xO_3$ systems [27]. These vacancies are produced due to loss of oxygen during sintering at high temperature in accordance with reaction [28]:

$$O_O \Leftrightarrow \frac{1}{2}O_2 + V_O^{\cdot\cdot} + 2e^{/} \tag{1}$$

where all the species are written in accordance with Kroger-Vink notation of defects [29]. These oxygen vacancies exist as doubly positively charged $V_O^{\cdot\cdot}$ above 850 K and as singly ionized, V_O at room temperature [30]. Singly positively charged oxygen vacancies will ionize as:

$$V_O^{\cdot\cdot} + e^{/} \Leftrightarrow V_O^{\cdot}(2) \tag{2}$$

at ~ 850 K.

In the present system both lanthanum and manganese are doped in equal concentration simultaneously. However, due to limitations of solid-state ceramic route, there will be some inhomogeneous mixing of these ions at microscopic level. This will lead to compensation of La^{3+} partly by vacancies on Ba^{2+} or Ti^{4+}. Similarly by Mn^{3+} on Ti^{4+} sites will be compensated by holes or oxygen vacancies. Oxygen vacancies are also produced due to loss of oxygen (reaction 1) which occurs during sintering in air [7, 27]. These singly or doubly positively charged oxygen vacancies may form defect complex's with Mn^{3+} or Mn^{2+} ions which are produced by capturing electrons from reaction (1); $Mn^{3+} + e^{/} \rightarrow Mn^{2+}$on Ti^{4+} sites as $V_o^{\blacksquare}$ -$Mn_{Ti}^{/}$ or $Mn_{Ti}^{//}$ -$V_o^{\blacksquare\blacksquare}$ as mentioned earlier based on ESR studies [6]. Presence of Mn on Ti site will lead to disrupting of Ti–O–Ti links responsible for ferroelectricity and hence lowering of T_C. This is in conformity with the observed results. Presence of lanthanum on Ba site will lead to generation of vacancies in Ti sublattice due to inhomogeneous mixing. This will also lead to lowering of T_C with increasing x.

Now let us consider the size of various ions. Mn^{2+} ion and Mn^{3+} have ionic radii of 0.645 Å (in high spin state) 0.82 Å as compared to 0.605 Å of Ti^{4+} ion, while La^{3+} ion has an ionic radius of 1.32 Å as compared to 1.60 Å of Ba^{2+} ion [31]. Majority of Mn ions are in +3 state as indicated by ESR studies along with a very small concentration of Mn^{2+} and Mn^{4+} ions [6]. Because of large difference in ionic radii for Ba^{2+} and La^{3+} sites, there will be distortion of (Ti, Mn) O_6 octahedra [26]. The observation of single anomaly in $x = 0.10$ at low temperature may be due to pinching effect of substituent ions similar to that observed in the case of only La doped barium titanate at a La concentration of 8 at% i.e. lowering of T_{C-T} is much faster as compared to T_{T-O} and T_{O-R} with increasing dopants concentration. A sharp decrease in resistivity is observed in $LaMnO_3$ at 723 K [32]. This is due to disappearance of Jahn–Teller distortion associated with Mn^{3+} ions. The anomaly appearing at ~490 K in ε_r versus T plot may be due to this transition which has been lowered because of Ba and Ti substitution [28]. In other compositions this may occur at higher temperatures which are beyond temperature range of measurements.

The result of present investigations show that effect of simultaneous substitution of La (on Ba-site) and Mn (on Ti-site) in equal concentration lead to decrease in Curie temperature. But decrease in Curie temperature has not been found to be systematic with composition as has been observed in the chromium doped system [33]. This seems due to interplay of variety of defects produced in this system which play a significant role to control the transition temperatures in ferroelectric materials. Thus the complete understanding of the effect of offvalent substitutions on the Curie temperature and dielectric properties of this system require more studies.

Conclusions

Solid solution forms in this system upto $x = 0.10$. Structure remains tetragonal upto $x \le 0.05$ and becomes cubic for

$x = 0.10$. The ratio of lattice parameters '*c*/*a*' is maximum for $x = 0.03$. Average grain size is small. All the dielectric anomalies corresponding to various phase transitions in $BaTiO_3$ have been found to decrease with increasing concentration of lanthanum and manganese in $BaTiO_3$. The observation of single anomaly in $x = 0.10$ may be due to pinching effect. At room temperature all these samples show low value of dielectric loss (0.05).

Acknowledgements Financial assistance from Department of Science and Technology, Government of India is gratefully acknowledged. We are grateful to Prof. D. Pandey for providing us X-ray diffraction facilities for these samples. We are thankful to Prof. T. K. Gundu Rao of I.I.T. Bombay for doing ESR spectra. Prakash Singh and Sindhu Singh are also grateful to C.S.I.R., New Delhi for providing financial assistance.

References

1. Jaffe B, Cook WR Jr, Jaffe H (1971) Piezoelectric ceramics. Academic Press, New York, p 91
2. Newnham RE (1983) J Mater Educ 5:941
3. Goodman G (1986) In: Buchanan RC (ed) Ceramic capacitor material. Marcel Dekker, Inc., New York, p 79
4. Daniels J, Hardtl KH (1976) Phillips Tech Rep 31:447
5. Shaikh AS, Vest RW (1986) J Am Ceram Soc 69(9):689
6. Jonker GH, Havinga EE (1982) Mater Res Bull 17:345
7. Bahadur D, Om Parkash (1983) J Solid State Chem 46:197
8. Om Parkash, Prasad CD, Kumar D (1989) Phys State Sol (a) 116:K81
9. Om Parkash, Prasad CD, Kumar D (1990) J Mater Sci 25:487
10. Om Parkash, Tare VB, Tewari HS, Kumar D (1993) J Phys D; Appl Phys 26:676
11. Om Parkash, Kumar D, Prasad CD (1994) J Phys D; Appl Phys 27:509
12. Upadhyay S, Kumar D, Om Parkash (1996) Bull Mater Sci 19:513
13. Om Parkash, Durga Prasad Ch, Kumar D (1991) J Mater Sci 102:203
14. Om Parkash, Tiwari HS, Pandey L, Kumar R, Kumar D (1989) J Am Ceram Soc 72:1520
15. Saito H, Chazono H, Kishi H, Yamaoka N (1991) Jpn J Appl Phys 30:2307
16. Takeuchi N, Abiru Y, Ishida S (2003) J Soc Mater Sci, Japan 52:1155
17. Takeuchi N, Monguchi O, Ishida S (2005) J Soc Mater Sci, Japan 54:767
18. Gilleo MA (1957) Acta Cryst 10:161
19. Goodenough JB, Longo JM (1970) Landolt-Bornstein Tabellen, vol 111/4a. Springer-Verlag, Berlin
20. Desu SB, Payne AD (1990) J Am Ceram Soc 73(11):3398
21. Kutty TRN (1986)Proc Ind Acad Sci 96:581
22. Shirane G, Hoshino S, Suzuki K (1950) Phys Rev 80:1705
23. Hippel AV (1995) Dielectrics and waves. New York, Wiley
24. Garcia D, Eiras JA (1991) Ferroelectrics 123:51
25. Mazdyasini KS, Brown LM (1971) J Am Ceram Soc 54(11):539
26. Morrison FD, Sinclair DC, West AR (1999) J Appl Phys 86(11):6355
27. Dwivedi RK, Om Parkash, Kumar D (2000) J Phys D; Appl Phys 33:88
28. Burn I, Neirman S (1982) J Mater Sci 17:3510
29. Kroger FA, Wink HJ (1956) Solid state physics. Academic Press, New York
30. Moos R, Hardtl KH (1997) J Am Ceram Soc 80:2549
31. Shanon RD, Prewitt CT (1969) Acta Cryst B25:925
32. Jonker JH (1966) J Appl Phys 37:1424
33. Dwivedi RK, Kumar D, Om Parkash, Srivastava KK, Singh P (in press) J Mater Sci